ChemComm

ROYAL SOCIETY OF CHEMISTRY

COMMUNICATION

View Article Online
View Journal | View Issue

Check for updates

Cite this: *Chem. Commun.*, 2020, **56**, 11062

Received 22nd June 2020,
Accepted 22nd July 2020

DOI: 10.1039/d0cc04334f

rsc.li/chemcomm

Heterotrimetallic {LnOVPt} complexes with antiferromagnetic Ln–V coupling and magnetic memory†

Stephanie A. Beach,[a] Jesse L. Guillet,[a] Sydney P. Lagueux,[a] Mauro Perfetti,[b] Brooke N. Livesay,[c] Matthew P. Shores,[c] Jeffrey W. Bacon,[a] Arnold L. Rheingold,[d] Polly L. Arnold‡§[e] and Linda H. Doerrer*[a]

The new $PtVO(SOCR)_4$ lantern complexes, 1 (R = CH_3) and 2 (R = Ph) behave as neutral O-donor ligands to $Ln(OR)_3$ with Ln = Ce, Nd. Four heterotrimetallic complexes with linear {LnOVPt} units were prepared: $[Ln(ODtbp)_3\{PtVO(SOCR)_4\}]$ (Ln = Ce, 3Ce (R = CH_3), 4Ce (R = Ph); Nd, 3Nd (R = CH_3), 4Nd (R = Ph); ODtbp = 2,6-ditertbutylphenolate). Magnetic characterization confirms slow magnetic relaxation behaviour and suggests antiferromagnetic coupling across {Ln–O=V} in all four complexes, with variations tunable as a function of Ln and R.

Rare earth elements have become essential in clean energy technologies such as the synthesis of batteries,[1] magnets,[2] and catalysts.[3] Due to the inherent magnetic anisotropy of these systems, lanthanide (Ln) complexes are best known for their potential single molecule magnet (SMM) behaviour which is used in the fields of molecular magnets and quantum information storage (QIS) technologies.[4] In the design of SMMs, low-coordinate Ln complexes with high anisotropy are preferred.[5,6] The coupling of d-block metals to Ln complexes is one strategy to increase the magnetic anisotropy of the system. Low coordinate 3d–4f complexes have been achieved with examples including an unsupported Nd–Fe bond[7] as well both ferro- and antiferromagnetic coupling in a vanadyl–Gd coupled complex.[8] More recently, focus has been on a bottom-up approach to the rational design of SMMs through structural and magnetic studies. While solvated LnX_3 complexes are very common, the formation of low coordinate species requires bulkier ligands such as substituted aryloxides, siloxides, and amides[9] with monodentate O-donor ligands being most common due to Ln oxophilicity. No coupling is observed in trinuclear LnM_2 complexes, but when arranged linearly, coupling is observed. Ligand geometry and different Ln ion f-orbital electron distributions (oblate or prolate) can also promote highly anisotropic ground states and greater coupling.[10] This phenomenon is exemplified in the magnetic coupling in dinuclear Tb(III)–Cu(II) complexes with O-donor ligands, which are tuned through ligand charge as well as the greater equatorial *vs.* axial ligand contributions to prolate Tb(III).[6]

In the present work, we set out to combine low coordinate lanthanide complexes with a vanadyl unit in an effort to effect magnetic coupling between d- and f-block metals. Design of linear M=O–Ln units is particularly needed since the majority of d-block-O–Ln adducts have used 4d/5d elements and result in diamond $\{Ln(\mu_2\text{-}O)M\}$ moieties. A variety of lantern complexes of the formula $[PtM(SOCR)_4(L)]$ (M = Mg, Ca, Cr, Mn, Fe, Co, Ni, Zn; R = CH_3 (SOCMe), Ph (SOCPh); L = substituted pyridines and donating solvents) are known.[11] Antiferromagnetic coupling of the 3d metals has been consistently observed in the solid state between staggered dimers through a metallophilic interaction. While the late transition metals have been studied in these systems, examples with early transition metals were lacking. We hypothesized that the Lewis basic {V=O} unit, which has already been shown to bind other metal centres,[12–14] would bind in a linear fashion to Ln. The only reported example of a vanadyl oxo forming a [Ln–O=V] unit is in the chiral visible-light photocatalyst cluster, $(nBu_4N)_2[(Ce(DMSO)_3)_2V^{IV}V^{V}{}_{11}O_{33}Cl]\cdot 2DMSO$, but magnetic coupling was not explored. Similarly, the majority of transition metals bound to lanthanides through an oxygen bridge are high

---

[a] Boston University, Department of Chemistry, 590 Commonwealth Ave, Boston, MA 02215, USA
[b] Department of Chemistry, University of Copenhagen, Universitetsparken 5, 2100 Copenhagen, Denmark
[c] Department of Chemistry, Colorado State University, Fort Collins, CO, 80523-1872, USA
[d] University of California, San Diego Department of Chemistry and Biochemistry, La Jolla, CA 92093, USA
[e] University of Edinburgh Joseph Black Building, David Brewster Road, Edinburgh, EH9 3FJ, UK

† Electronic supplementary information (ESI) available. CCDC 2010910–2010915. For ESI and crystallographic data in CIF or other electronic format see DOI: 10.1039/d0cc04334f

‡ Current address: Department of Chemistry, University of California, Berkeley, CA 94720, USA. E-mail: pla@berkeley.edu

§ Current address: Chemical Sciences Division, Lawrence Berkeley National Laboratory, Berkeley, CA94720, USA.

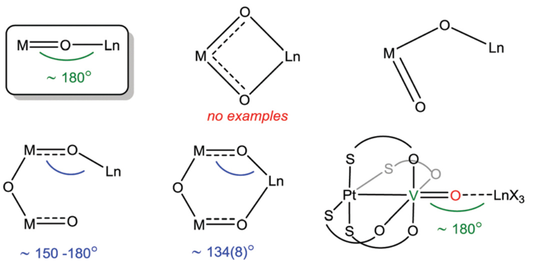

Scheme 1 Known Ln–O–M patterns (M= transition metal) and lantern binding mode.

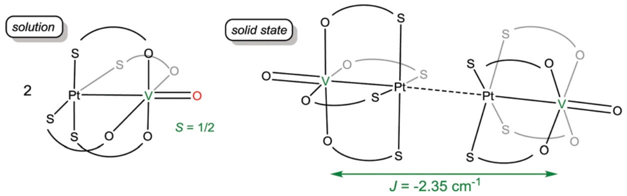

Scheme 2 Solution and solid-state structure for **1**.

coordinate polyoxometalates (M = Mo,W, Re) bound through a metal oxo unit that is rarely linear and by definition does not have a single transition metal center.[15–18] Both linear and bent binding of a uranyl oxo[19] to Ln has been reported and strong antiferromagnetic coupling exists in a U(V)Sm(III) monomer, whereas a U(V)Dy(III) dimer shows magnetic bistability at 3 K.[20] As seen in Scheme 1, the majority of known M=O–Ln linkages are bent, whereas a {V=O} lantern can uniquely favour an anisotropic environment and prevent the coordination of other {MO} units.

Anisotropic {V=O}-containing lanterns [PtVO(SOCMe)$_4$] (**1**) and [PtVO(SOCPh)$_4$] (**2**) were synthesized similarly to our previously published complexes using VOSO$_4$ as the starting V(IV) source.[11] Rather than forming 1D chains in the solid state, with the terminal oxo interacting with the {PtM} σ^* orbital of an adjacent lantern, as seen with an S^N donor ligand,[14] both **1** and **2** form dimers in the solid state with different intermolecular interactions. Complex **1** forms a staggered dimer ($\sim D_{4d}$) in which the intermolecular Pt···Pt distances of 3.1747(5) Å are shorter than the resultant Pt···S contacts and the thiocarboxylate backbones are staggered when viewed along the metal axis (Fig. S1, ESI†). In comparison, **2** forms a square dimer ($\sim D_{2h}$) (Fig. S2 and S3, ESI†) in the solid state, dominated by a close intermolecular Pt···S contact of 3.126(2) Å, rather than a metallophilic interaction or any interdimer coupling (Table S1, ESI†).

Solution phase Evans method[21,22] magnetic moment measurements yielded μ_{eff} values of 1.68 (**1**) and 1.60 (**2**), consistent with the predicted spin-only magnetic moment (1.73) of reported V(IV) complexes with tetradentate ONNO ligands.[23,24] Shown in Fig. S9 (ESI†), the solid state magnetic susceptibility temperature product of staggered dimer **1** at room temperature (χT = 0.839 cm^3 K mol^{-1}) is higher than two magnetically uncoupled V(IV) centres (0.75 cm^3 K mol^{-1} for g = 2); however, below 10 K, the $\chi_{\mathrm{M}}T$ product shows a sharp decrease (0.103 cm^3 K mol^{-1}). Fitting these data leads to an exchange coupling of $J = -2.35$ cm^{-1}, suggesting antiferromagnetic coupling between V(IV) ions in adjacent complexes (Fig. S1, ESI†) with competing interactions from other close neighbors indicated in the higher-than-expected Weiss constant calculated from the temperature dependence of 1/χ (Fig. S5, ESI†). Whether this is due to communication *via* a Pt–Pt contact (Scheme 2) or through space (Fig. S1, ESI†) cannot be determined definitively. Certainly, the near orthogonality of the magnetic (d$_{xy}$) orbitals in the staggered dimer is consistent with the observation of weak exchange coupling. Details for the magnetic exchange interpretation are provided in the ESI.† In sum, both **1** and **2** chemically act as monomers in solution (Scheme 2) and can be tested as discrete monodentate ligands for coordination to Ln ions.

Lanthanide tris-aryloxide complexes, particularly the 2,6-ditertbutylphenolate derivatives (Ln(ODtbp)$_3$ where Ln = Ce, Nd), have previously served as starting materials in non-donor solvents.[9,25,26] When green toluene solutions of either **1** or **2** and Ln(Odtbp)$_3$ (Ce = yellow, Nd = blue) are mixed, an immediate colour change to a dark brown/red is observed in all four cases. Air-sensitive, analytically pure, X-ray quality material was grown from the reaction mixtures and isolated in high yield (~80%). For full synthetic and characterization details, see ESI.†

Structural characterization of the products of these reactions revealed the successful coordination of one equivalent of **1** or **2** to both Ce(ODtbp)$_3$ and Nd(ODtbp)$_3$, giving [Ce(ODtbp)$_3${PtVO(SOCMe)$_4$}] (**3Ce**), [Ce(ODtbp)$_3${PtVO(SOCPh)$_4$}] (**4Ce**), [Nd(ODtbp)$_3${PtVO(SOCMe)$_4$}] (**3Nd**), and [Nd(ODtbp)$_3${PtVO(SOCPh)$_4$}] (**4Nd**). As exemplified by **3Ce**, shown in Fig. 1, these complexes feature coordination of the lantern complex to the Ln center through the {V=O}, resulting in pseudo-tetrahedral geometry about Ln.

The {V=O} stretching frequency shifts from 983 cm^{-1} in **1** to 912 cm^{-1} in **3Ce** and **3Nd** and from 953 cm^{-1} in **2** to 911 cm^{-1} in **4Ce** and **4Nd**, respectively (Fig. S10–S12, ESI†), consistent with the weakening of the V–O bonding interaction upon Ln coordination. These values are consistent with extensive prior IR characterization of {V=O} units,[27] in the range of 900–1050 cm^{-1}.

Blue shifts are observed for the d–d transitions of 580 nm and 593 nm in **3Nd** and 583 nm and 595 nm in **4Nd** when compared to the unbound **1** (607 nm and 712 nm) and **2** (628 nm and 726 nm), respectively (Fig. S13–S15, ESI†). In **3Ce** and **4Ce**, however, the broad f–d transitions between 400–600 nm are

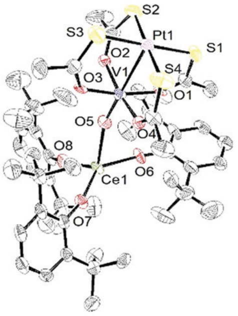

Fig. 1 ORTEP of [Ce(ODtbp)$_3${PtVO(SOCMe)$_4$}] (**3Ce**). Ellipsoids shown at the 50% level. Hydrogen atoms and solvent molecules excluded for clarity.

Table 1 Selected bond distances (Å) and angles (°) of **1**, **2**, **3Ln**, and **4Ln**

	Pt–V (Å)	V–O (Å)	Pt–VO (°)	Ln–OV (Å)	Pt–VO (°)	Ln–OV (°)	O–V–Pt–S torsion (avg)
1	2.8635(6)	1.592(2)	179.7(1)	N/A	179.7(1)	N/A	15.19
2	2.782(1)	1.581(4)	179.8(1)	N/A	179.8(1)	N/A	20.65
3Ce	2.768(1)	1.630(3)	178.6(1)	2.455(4)	178.6(1)	163.7(2)	5.8
4Ce-a	2.7878(9)	1.682(3)	179.0(1)	2.525(3)	179.0(1)	174.4(2)	4.35
4Ce-b	2.7653(9)	1.616(3)	179.4(1)	2.531(3)	179.4(1)	175.8(2)	18.7
3Nd	2.762(1)	1.625(5)	176.7(2)	2.438(5)	176.7(2)	164.8(3)	15.4
5Nd-a	2.7604(6)	1.629(2)	179.37(9)	2.470(2)	179.37(9)	174.2(1)	19.3
5Nd-b	2.7861(6)	1.630(2)	178.99(9)	2.477(2)	178.99(9)	173.6(1)	15.6

strong enough to prevent the weak d–d transitions from being observed (Fig. S16 and S17, ESI†).

All six complexes have been characterized *via* single crystal X-ray diffraction. Important metrical data are collected in Table 1. As previously mentioned, **1** and **2** form dimers in the solid state that do not persist in solution. In the SOCMe-containing **3Ce** and **3Nd**, a slight increase in {V═O} bond distances accompanied by a decrease in {Pt–V} is observed while maintaining a largely linear Pt–VO angle. These changes are consistent with reduction in {V═O} π-bond character, and increased Lewis acidity at V that draws Pt closer. In SOCPh-containing **4Ce** and **4Nd**, there are two independent molecules in the asymmetric unit, denoted as **4Ce-a/b** and **4Nd-a/b**. When comparing **4Ce** and **4Nd** to unbound **2**, the same increase in {V═O} distance is observed but with a smaller decrease in the {Pt–V} bond length than in **3Ce** and **3Nd**.

The complexes were characterized using DC magnetometry. The Curie constant for a V(IV) ion (0.375 emu K mol^{-1}) plus that of the Ln(III) ion (Ce^{3+} = 0.8 emu K mol^{-1}, Nd^{3+} = 1.64 emu K mol^{-1}) are 1.175 emu K mol^{-1} and 2.015 emu K mol^{-1}, respectively (see dashed lines in Fig. 2). The experimental curves reach values extremely close: 1.176 (**3Ce**), 1.176 (**4Ce**), 2.019 (**3Nd**), 2.000 (**4Nd**), confirming the retained oxidation states of V(IV) and Ln(III) in these air-sensitive samples. These data also indicate a relatively small crystal field (CF) splitting, as expected for 4f complexes with pseudo-tetrahedral geometries. Each complex shows a sharp decrease in χT at low T that when compared to the *M vs. H* curves (Fig. S18, ESI†), indicates either CF splitting and/or possible weak antiferromagnetic interactions of the Ln(III) and V(IV) ions.

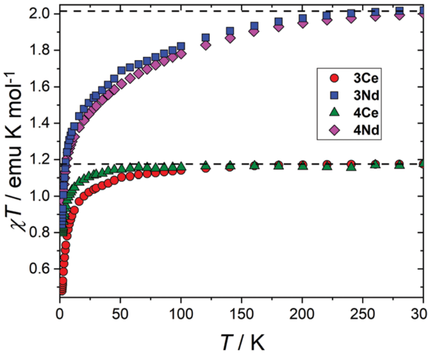

Fig. 2 Product of the magnetic susceptibility times the temperature *vs.* the temperature for **3Ln** and **4Ln**. The black dashed lines are the expected Curie constants for independent V(IV) and Ln(III) ions.

Compound **4Ce** shows the lowest decrease in χT at low temperatures and has the most well-isolated ground state (see the *M vs. H*/*T* curves in Fig. S19, ESI†). Interestingly, **3Nd** and **4Ln** reach a very similar χT value at the lowest temperature (0.8–0.9 emu K mol^{-1}), while compound **3Ce** drops to 0.45 emu K mol^{-1}. This suggests that either the CF around the Ln stabilizes the same ground state in **3Nd** and **4Ln**, but a different one in **3Ce** or, more likely, the antiferromagnetic interactions in **3Ce** are significantly higher than in the other three compounds. The better coupling in **3Ce** which has the smaller SAc containing lantern paired with the larger ionic radii of Ce(III), confirms the previously discussed importance of ligand size and geometry. To promote better coupling, the steric bulk of the lantern or aryloxides would need to be decreased to allow for closer {VO} contact to the Ln. Unfortunately, the measured data are not suitable for a quantitative evaluation due to an over parametrization and correlation problem which is impossible to overcome without *ab initio* calculations or a large span of spectroscopic techniques.[28] Indeed, for these systems a reasonable fit must include too many parameters (*e.g.* the CF parameters of the Ln, the Ln–V coupling, the g value of V), that are also difficult to disentangle using only magnetic data.

The metrical parameters of greatest interest are the Ln–O distances and Ln–O–V angles. Depending on the shape of the Ln ion (oblate or prolate), certain ligand environments can stabilize the electron distribution and therefore promote the desired coupling.[10] In the cases of Ce(III) and Nd(III) which are both oblate, strong axial ligand donation is most effective for the stabilization of a high projection of the total angular momentum. In all cases the axial-like Ln–O$_{\text{lantern}}$ distances of **3Ln** and **4Ln** are the longest (2.44–2.53 Å) while the equatorial-like Ln–O$_{\text{ODtbp}}$ lengths are shortest (2.14–2.22 Å). These data suggest that the CF around the Ln in these complexes does not effectively stabilize the highest projection of the total angular momentum, thus hinting towards poor slow relaxation behaviour.

The dynamic magnetic behaviour of **3Ln** and **4Ln** have been tested using AC susceptibility measurements. When an external DC field is applied to quench tunnelling and any other relaxation pathways that could lower the effective barrier for the relaxation of the magnetisation, all four complexes presented a frequency dependent AC signal with the SOCPh derivatives **4Ce** and **4Nd** being more intense (see Fig. 3) than the SOCMe derivatives (Fig. S20, ESI†). This suggests a significantly different ligand field for the two employed lanterns. The longest relaxation time is observed in **3Nd**, with a value of *ca.* 0.16 ms at T = 2 K and H = 5000 Oe. However, in all cases, the full peak is

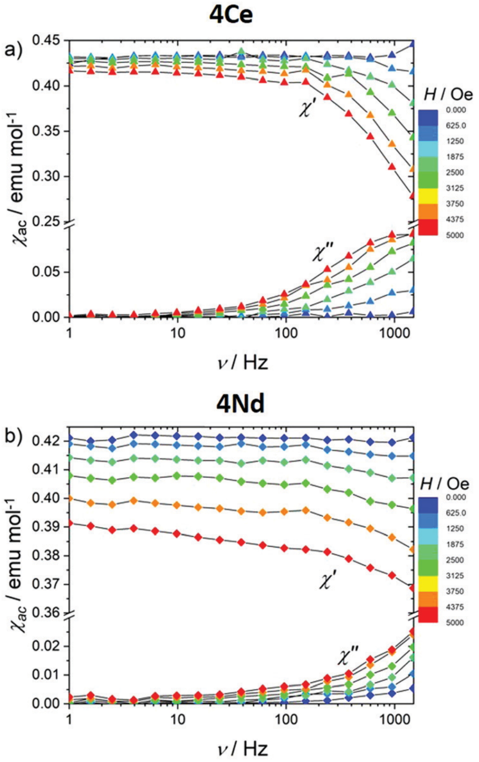

Fig. 3 AC magnetic susceptibility of (a) **4Ce** and (b) **4Nd** obtained at T = 2 K and different applied DC fields.

outside the range of experimental frequencies at the lowest possible temperature (2 K), preventing further investigation.

In summary, two new $S = 1/2$ [PtVO(SOCR)$_4$] lantern complexes, **1** (R=Me) and **2** (R=Ph), have been synthesized and magnetically characterized, confirming $S = 1/2$ ground states. The monomeric lanterns act as ligands for low coordinate Ln(ODtbp)$_3$ in new four-coordinate heterotrimetallic {LnOVPt} compounds: [Ln(ODtbp)$_3${PtVO(SOCR)$_4$}] (Ln = Ce), **3Ce** (R = CH$_3$), **4Ce** (R = Ph); Nd, **3Nd** (R = CH$_3$), **4Nd** (R = Ph). AC susceptibility measurements show weak slow magnetic relaxation behaviour in **3Ln** and **4Ln**, with each ligand type (SOCMe *vs.* SOCPh) leading to significantly different ligand fields about the Ln, with the slowest relaxation time observed in **3Nd.** Variable-temperature susceptibility measurements suggested antiferromagnetic coupling to be strongest in **3Ce**, which contains the less bulky SAc lantern and larger Ce(III) ionic radius, hinting that a move to generally less bulky ligands should promote even greater antiferromagnetic coupling in future {Ce–OV} complexes for potential quantum information science systems despite the weaker slow relaxation behaviour.

The authors thank the Royal Society of Chemistry's Researchers Mobility Grant (SAB) and Boston University UROP (SPL). M. P. thanks Prof. Jesper Bendix for giving access to the SQUID magnetometer. M. P. S. and B. N. L. acknowledge NSF (CHE 1363274, 1800554 and 1956399) for support of magnetic measurement capabilities. We thank Dr Rory Kelly for helpful discussions. Additional discussion, analysis, and writing of this manuscript (PLA) was supported by the U.S. Department of Energy (DOE), Office of Science, Office of Basic Energy Sciences, Chemical Sciences, Geosciences, and Biosciences Division at the Lawrence Berkeley National Laboratory under Contract DE-AC02-05CH1123.

Conflicts of interest

There are no conflicts to declare.

Notes and references

1 J. Xia, H. Zhao, W. K. Pang, Z. Yin, B. Zhou, G. He, Z. Guo and Y. Du, *Chem. Sci.*, 2018, **9**, 3421–3425.
2 F.-S. Guo, B. M. Day, Y.-C. Chen, M.-L. Tong, A. Mansikkamäki and R. A. Layfield, *Science*, 2018, eaav0652, DOI: 10.1126/science.aav0652.
3 P. L. Arnold and Z. R. Turner, *Nat. Rev. Chem.*, 2017, **1**, 0002.
4 C. Benelli and D. Gatteschi, *Introduction to molecular magnetism: From transition metals to lanthanides*, John Wiley & Sons, 2015.
5 D. N. Woodruff, R. E. P. Winpenny and R. A. Layfield, *Chem. Rev.*, 2013, **113**, 5110–5148.
6 K. Liu, W. Shi and P. Cheng, *Coord. Chem. Rev.*, 2015, **289–290**, 74–122.
7 P. L. Arnold, J. McMaster and S. T. Liddle, *Chem. Commun.*, 2009, 818–820, DOI: 10.1039/B819072K.
8 R. Watanabe, K. Fujiwara, A. Okazawa, G. Tanaka, S. Yoshii, H. Nojiri and T. Ishida, *Chem. Commun.*, 2011, **47**, 2110–2112.
9 P. B. Hitchcock, M. F. Lappert and A. Singh, *J. Chem. Soc., Chem. Commun.*, 1983, 1499–1501.
10 J. D. Rinehart and J. R. Long, *Chem. Sci.*, 2011, **2**, 2078–2085.
11 S. A. Beach and L. H. Doerrer, *Acc. Chem. Res.*, 2018, **51**, 1063–1072.
12 H.-J. Koo and M.-H. Whangbo, *Solid State Sci.*, 2010, **12**, 685–690.
13 C. Weeks, Y. Song, M. Suzuki, N. A. Chernova, P. Y. Zavalij and M. S. Whittingham, *J. Mater. Chem.*, 2003, **13**, 1420–1423.
14 K. i. Kitano, R. Tanaka, T. Kimura, T. Tsuda, S. Shimizu, H. Takagi, T. Nishioka, D. Shiomi, A. Ichimura, I. Kinoshita, K. Isobe and S. i. Ooi, *Dalton*, 2000, 995–1000.
15 T. Ishida, R. Watanabe, K. Fujiwara, A. Okazawa, N. Kojima, G. Tanaka, S. Yoshii and H. Nojiri, *Dalton Trans.*, 2012, **41**, 13609–13619.
16 J. P. Costes, F. Dahan, A. Dupuis and J. P. Laurent, *Chem. – Eur. J.*, 1998, **4**, 1616–1620.
17 J. M. Cameron, G. N. Newton, C. Busche, D.-L. Long, H. Oshio and L. Cronin, *Chem. Commun.*, 2013, **49**, 3395–3397.
18 K.-L. Wong, Y.-M. So, G.-C. Wang, H. H.-Y. Sung, I. D. Williams and W.-H. Leung, *Dalton Trans.*, 2016, **45**, 8770–8776.
19 P. L. Arnold, E. Hollis, F. J. White, N. Magnani, R. Caciuffo and J. B. Love, *Angew. Chem.*, 2011, **123**, 917–920.
20 P. L. Arnold, E. Hollis, G. S. Nichol, J. B. Love, J.-C. Griveau, R. Caciuffo, N. Magnani, L. Maron, L. Castro, A. Yahia, S. O. Odoh and G. Schreckenbach, *J. Am. Chem. Soc.*, 2013, **135**, 3841–3854.
21 D. F. Evans, *J. Chem. Soc.*, 1959, 2003–2005.
22 S. K. Sur, *J. Magn. Reson.*, 1989, **82**, 169–173.
23 M. Sutradhar, G. Mukherjee, M. G. B. Drew and S. Ghosh, *Inorg. Chem.*, 2007, **46**, 5069–5075.
24 P. Pattanayak, J. L. Pratihar, D. Patra, S. Mitra, A. Bhattacharyya, H. Man Lee and S. Chattopadhyay, *Dalton Trans.*, 2009, 6220–6230, DOI: 10.1039/B903352A.
25 H. A. Stecher, A. Sen and A. L. Rheingold, *Inorg. Chem.*, 1988, **27**, 1130–1132.
26 H. D. Amberger, H. Reddmann, C. Guttenberger, B. Unrecht, L. Zhang, C. Apostolidis, O. Walter and B. Kanellakopulos, *Z. Anorg. Allg. Chem.*, 2003, **629**, 1522–1534.
27 J. Selbin, *Coord. Chem. Rev.*, 1966, **1**, 293–314.
28 M. Perfetti, M. Gysler, Y. Rechkemmer-Patalen, P. Zhang, H. Taştan, F. Fischer, J. Netz, W. Frey, L. W. Zimmermann, T. Schleid, M. Hakl, M. Orlita, L. Ungur, L. Chibotaru, T. Brock-Nannestad, S. Piligkos and J. van Slageren, *Chem. Sci.*, 2019, **10**, 2101–2110.